Int. J. Adv. Appl. Math. and Mech. 11(2) (2023) 53 – 64 (ISSN: 2347-2529)
Journal homepage: www.ijaamm.com

International Journal of Advances in Applied Mathematics and Mechanics

Investigation of air pollution due to agrochemicals over large farms by k-ϵ turbulence model

Research Article

Kihuga Daniel Kariuki[a, *], Kinyanjui Matthew Ngugi[b], Kimathi Mark Eric Mwiti[c]

[a] *Pan African University Institute for Basic Sciences Technology and Innovation (PAUSTI), Nairobi, Kenya*
[b] *Department of Pure and Applied Mathematics, Jomo Kenyatta University of Agriculture and Technology (JKUAT), Nairobi, Kenya*
[c] *School of Pure and Applied Sciences, Machakos University (MKSU), Machakos, Kenya*

Received 11 June 2023; accepted (in revised version) 12 July 2023

Abstract: In recent years, air pollution has received serious concerns from researchers, media, and the public sectors, but air pollution from agricultural production activities has not received enough attention. This paper focuses on agricultural air pollution in Naivasha-Kenya, which is aggravated by the ongoing large scale horticultural practices where high usage of agrochemicals is experienced. The k-ϵ turbulence model was simulated to model wind velocities and pollutant dispersion subjected to vegetation. The model coupled convection-diffusion equation where particles released are influenced by the wind flow. The study was aimed at determining the pollutants concentration, the effects of Schmidt number and vegetation cover,kinetic energy and dissipation within the flow. The nonlinear partial differential equation governing the flow were solved numerically using the finite difference method and implemented in MATLAB. The results obtained were presented in tables and graphs. The observations were discussed on the effects of varying various parameters and vegetation factor on the pollutants concentration, kinetic energy and dissipation. Results for the examined mesh densities indicated that high agrochemicals concentration were observed at the position with high vegetation factor. The kinetic energy was significantly affected by increased velocities. It was also observed that increased Schmidt numbers reduces agrochemicals concentration and decrease in the number increases the pollutants concentration. The results provide useful information to the environmentalist to improve air quality through policy making and medical practitioners in treatments.

MSC: 76F60 • 65D17

Keywords: Agrochemicals Concentration • Kinetic energy • Dissipation

1. Introduction

Population growth and climate change contribute mainly to the increasing use of pesticides [1], and a higher global pesticide production is estimated in the future. Although agrochemicals play a significant role in improving crop yields and the production of affordable and good quality food, the increasing use of agrochemicals also brings a number of negative effects to the environment and human health [2]. Agrochemicals are used to kill pests and control weeds as a function of their chemical ingredients, therefore, they can also be toxic to other organisms. Such chemical residues impact human health through the environment and food contamination. Moreover, Agrochemical contamination

* Corresponding author.
E-mail address(es): kihugadaniel36@gmail.com (Kihuga Daniel Kariuki), mathewkiny@jkuat.ac.ke (Kinyanjui Matthew Ngugi), memkimathi@gmail.com (Kimathi Mark Eric Mwiti).

moves away from the target plants, resulting in environmental pollution. Agrochemicals move in several ways, including to the air, through wind currents, to water and soil, through run-off or leaching, and to plants, animals, and humans.

The research narrows to air pollution and therefore the need to understand what air pollution is and how it takes place in our environment. Air pollution is when gases, dust particles, fumes (smoke) or odour are introduced into the atmosphere in a way that makes it harmful to humans, animals and plant. Pollutants from agrochemical such as fertilizers, herbicides and pesticides are introduced into the environment by spraying over the agricultural farms. Example of agronomic practices are shown photos as in the figure 1 where drones are used to spray agrochemicals which are harmful to human health.

Fig. 1. Agriculture drone fly to sprayed fertilizer on the green tea fields, Source:Wikipedia

An agricultural aircraft is an aircraft that has been built or converted for agricultural use – usually aerial application of pesticides (crop dusting) or fertilizer (aerial topdressing); in these roles they are referred to as "crop dusters" or "top dressers". Agricultural aircraft are also used for hydroseeding where the figure 2 shows such a plane spraying agrochemicals.

Fig. 2. Agricultural aircraft spraying agrochemicals on a farm- Source:Wikipedia

Climate change, increasing population growth, emergence of crop diseases, damages to crops from rodents and critters, and shrinking farming land in some regions are among challenges global agriculture sector faces. The application of agrochemicals in such ways has proven to be an efficient answer to some of these challenges [3]. Air is one of the primary mechanisms by which pesticides are transported from targeted application areas to other parts of the environment and, thus, there is potential for movement into and through all components of the hydrologic cycle. The atmosphere is recognized as a major pathway by which pesticides and other organic and inorganic compounds are transported and deposited in areas sometimes far removed from their sources. The study focuses on the dispersion of agrochemical pollutants that affect human health through air by k-ϵ turbulence model.

2. Literature

Even though clean air is considered as a basic requirement for the maintenance of human health, air pollution continues to pose a significant health threat in developed and developing countries alike. Monitoring and modeling of classic and emerging pollutants is vital to our knowledge of health outcomes in exposed subjects and to our ability to predict them. The ability to anticipate and manage changes in atmospheric pollutant concentrations relies on an accurate representation of the chemical state of the atmosphere[4]. The task of providing the best possible analysis of air pollution thus requires efficient computational tools enabling efficient integration of observational data into models.

The atmosphere is an important component of the hydrologic cycle to consider in assessing the effect of pesticides in the environment. Pesticides have been recognized as potential air pollutants since 1940(s). Long-range movement of pesticides was thought to be minimal, if any, because of their physical and chemical properties. A national perspective on the occurrence and geographical distribution of pesticides in the atmosphere was developed from the observations reported in the reviewed studies, with particular emphasis on the large-scale studies [6].

Investigation on how spraying configuration could contribute the reduction of spray losses in the context of sustainable agriculture was studied by [3] through three themes. The first theme introduced a method for fluid quantification from a sprayer jet using a Particle Image Velocimetry (PIV) system in combination with imaging processing. The second theme investigated the velocity distribution of an extended flat fan nozzle to determine the weak jet areas, which have high risks of droplet drift, using the Particle Image Velocimetry (PIV) method and Computational Fluid Dynamics (CFD) with volume of fluid (VOF) simulation approach. The third theme dealt with the development of a mathematical model to jointly minimize spraying time and drift losses. The results showed that valid and reasonable solutions would be obtained by selecting the appropriate combination of boom height, nozzle spacing, nozzle type and tractor travel speed.

Open field burning of crop residue has been intentionally prohibited due to the undesired air pollution in urban regions. A feasibility study of prescribed burning for crop residues based on air quality assessment in urban regions was conducted by [5]. They established emission inventories using the top-down approach based on designed subregional fire as prescribed burning whereas air qualities in urban regions were simulated by the coupled Weather Research and Forecasting Model-Community Multi-scale Air Quality Model (WRF-CMAQ) covering different sensitivity experiments. It was revealed that prescribed burning would achieve highly efficient disposal of crop residues under the premise of ensuring the air quality in urban regions.

Air-assisted sprayer can effectively promote the deformation of tree leaves and improve the deposition performance of droplets in the target canopy interior with the help of strong assisted airflow. In their study, [7] selected the grape leaves as the research object to clarify the deformation behavior of leaves under the assisted airflow. They established a bidirectional fluid–structure interaction model using computational fluid dynamics (CFD) based on the measurement of leaves parameters. The model was verified by a high-speed camera, and the maximum deformation of leaves centroid and tip in CFD simulation were compared with the shooting results. They concluded that the research results provided a reference for the regulation and optimization of the pneumatic system of sprayers.

Agricultural drones are transforming on the way farming is being carried out. They are very suitable and agile for working in a large area of land and rough terrains with high efficiency. According to [8],they can increase and improve the efficiency of spraying more area of land in a shorter duration compared to a knapsack sprayer. They designed the entire research based on quantitative research, which was conducted through simulation using SolidWorks, MATLAB and Ansys Fluent. SolidWorks was used for planning, modelling and visual ideation of the agricultural drone. MATLAB was used to simulate the agricultural drone to fly in a specific pattern to water a certain area. Velocity, acceleration, position and flight pathway graphs were plotted. These data were collected to observe how evenly the entire area being sprayed is fully covered. Ansys Fluent was used to display the velocity that the fluid will be flowing inside the nozzle and spraying it out.

Multicopter flow fields and their influence on a spray released from multicopters was studied by [9]. Multicopters are remote-controlled vertical take-off and landing unpiloted aerial vehicles (UAVs). They considered to understanding the behaviour of spray crucial for targeted spray dispersal and for the protection of sensitive areas. They studied multicopter wake and its influence on the performance of spraying liquid. The primary experimental technique used for the study of multicopter wake was stereo particle image velocimetry (SPIV), supplemented by constant temperature anemometry (CTA) with a three-axial probe. The model can be used to evaluate the swath pattern left on the ground by the multicopter. It showed acceptable validity for hovering flight and flight velocities of up to 2.8-5 m/s when flight parameters can be approximately estimated.

Environment that comprised by unpolluted air, water, soil, far from noise and other dirtiness, clean, beautiful, green and healthy is the biggest demand of present day human and guarantee of future. This research was to investigation air pollution due to agrochemicals over large farms by k-ϵ turbulence model and mitigation factors on settlement setup through vegetation cover.

3. Mathematical formulation

The equations governing study of turbulent flows are formulated. The continuity, momentum, concentration and the energy equations together with k-ϵ equations are used in this work. These governing equations are those that facilitate the analysis of pollutants dispersion which forms the basis of our interest in studying the dispersion of agrochemicals from large farms to the residential areas. The governing equations used in this paper are those that govern turbulent flows since we consider to model the dispersion of agrochemical through wind. Therefore, the general mean flow equations for the compressible turbulent flows where effects of density fluctuations are negligible are as given below;

$$\frac{\partial \overline{\rho}}{\partial t} + div\vec{u} = 0 \tag{1}$$

$$\frac{\partial(\overline{\rho}u)}{\partial t} + \nabla(\overline{\rho}u\vec{u}) = -\frac{\partial p}{\partial x} + \mu\nabla.(\nabla(u)) + \left[\frac{\partial(\overline{-\overline{\rho}u'^2})}{\partial x} + \frac{\partial(\overline{-\overline{\rho}u'v'})}{\partial y} + \frac{\partial(\overline{-\overline{\rho}u'w'})}{\partial z}\right] + S_{mx} \tag{2}$$

$$\frac{\partial(\overline{\rho}v)}{\partial t} + \nabla(\overline{\rho}v\vec{u}) = -\frac{\partial p}{\partial y} + \mu\nabla.(\nabla(v)) + \left[\frac{\partial(\overline{-\overline{\rho}u'v'})}{\partial x} + \frac{\partial(\overline{-\overline{\rho}v'^2})}{\partial y} + \frac{\partial(\overline{-\overline{\rho}v'w'})}{\partial z}\right] + S_{my} \tag{3}$$

$$\frac{\partial(\overline{\rho}w)}{\partial t} + \nabla(\overline{\rho}w\vec{u}) = -\frac{\partial p}{\partial z} + \mu\nabla.(\nabla(w)) + \left[\frac{\partial(\overline{-\overline{\rho}u'w'})}{\partial x} + \frac{\partial(\overline{-\overline{\rho}v'w'})}{\partial y} + \frac{\partial(\overline{-\overline{\rho}w'^2})}{\partial z}\right] + S_{mz} \tag{4}$$

And the general scalar transport equation is as follows;

$$\frac{\partial(\overline{\rho}\Phi)}{\partial t} + \nabla(\overline{\rho}\Phi\vec{u}) = \nabla.(\Gamma_\Phi\nabla(\Phi)) + \left[\frac{\partial(\overline{-\overline{\rho}u'\varphi'})}{\partial x} + \frac{\partial(\overline{-\overline{\rho}v'\varphi'})}{\partial y} + \frac{\partial(\overline{-\overline{\rho}w'\varphi'})}{\partial z}\right] + S_\Phi \tag{5}$$

we apply the general scalar transport equation on to the concentration and the temperature equation as follows;

$$\frac{\partial c}{\partial t} + \nabla.(\vec{u}c) = \nabla.(D\nabla c) + \left[\frac{\partial(\overline{-u'c'})}{\partial x} + \frac{\partial(\overline{-v'c'})}{\partial y} + \frac{\partial(\overline{-w'c'})}{\partial z}\right] + \mathbf{S} \tag{6}$$

$$\rho C_p\left(\frac{\partial T}{\partial t} + \nabla.(\vec{u}T)\right) = \nabla.(ke\nabla T) + \left[\frac{\partial(\overline{-u'T'})}{\partial x} + \frac{\partial(\overline{-v'T'})}{\partial y} + \frac{\partial(\overline{-w'T'})}{\partial z}\right] + \mu\phi \tag{7}$$

The derived k-ϵ model equations were as given below where the dissipation equation mimics the kinetic energy equation.

$$\frac{\partial k}{\partial t} + u_j\frac{\partial k}{\partial x_j} = \frac{\mu_t}{\rho}S^2 - \epsilon + \frac{\partial}{\partial x_j}\left[\frac{1}{\rho}\left(\mu + \frac{\mu_t}{\sigma_k}\right)\frac{\partial k}{\partial x_j}\right] \tag{8}$$

$$\frac{\partial \epsilon}{\partial t} + u_j\frac{\partial \epsilon}{\partial x_j} = \frac{\epsilon}{k}\left(C_{1\epsilon}\frac{\mu_t}{\rho}S^2 - C_{2\epsilon}\epsilon\right) + \frac{\partial}{\partial x_j}\left[\frac{1}{\rho}\left(\rho + \frac{\mu_t}{\sigma_\epsilon}\right)\frac{\partial \epsilon}{\partial x_j}\right] \tag{9}$$

For the averaged Navier Stoke equations, the averaged concentration equation and averaged temperature equation i.e. equations 1 to 4, equation 6 and 7 the Boussinesq approximation, equation 10 was used to eliminate the turbulence stochastic nature of the terms on the right hand side(RHS);

$$-\rho\overline{u_i'u_j'} = \mu_t\left(\frac{\partial u_i}{\partial x_j} + \frac{\partial u_j}{\partial x_i}\right) - \frac{2}{3}\rho k\delta_{ij} \tag{10}$$

4. Methodology

Modelling the wind and temperature effects on agrochemicals concentration in the atmosphere over agronomic fields was considered where the $k-\epsilon$ model equations were applied. The approximation of wind velocities, temperature, kinetic energy, dissipation variations,and pollutant concentration in the environment were obtained. The geometry of the mathematical model considered was as shown in the figure 3 below.

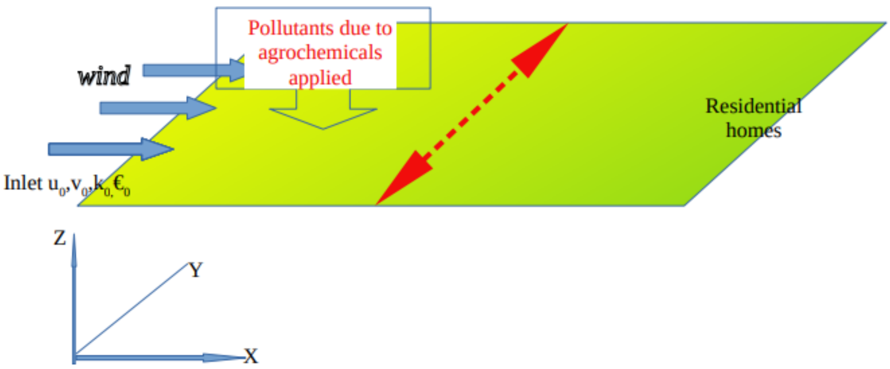

Fig. 3. Geometry of the mathematical model used

with reference to the mathematical geometry, figure 3 while making the assumptions that at specific height; density, pressure difference and specific heat are constants, yet fluid inertia forces are infinitely small compared to viscous force and that dispersion of agrochemical pollutants only depend on fluid velocities and coriolis forces and by use of the Boussinesq approximation equation 10, the equations 1 to 4; and equations 6 and 7 were reduced to the equations below together with the $k-\epsilon$ model equations;

$$\frac{\partial u}{\partial t}+v\frac{\partial u}{\partial y}=-\frac{1}{\rho}\frac{\partial p}{\partial x}+\frac{\mu+\mu_t}{\rho}\left(\frac{\partial^2 u}{\partial x^2}+\frac{\partial^2 u}{\partial y^2}\right)+S_{mx}+fc \tag{11}$$

$$\frac{\partial v}{\partial t}+u\frac{\partial v}{\partial x}=-\frac{1}{\rho}\frac{\partial p}{\partial y}+\frac{\mu+\mu_t}{\rho}\left(\frac{\partial^2 v}{\partial x^2}+\frac{\partial^2 v}{\partial y^2}\right)+S_{my}+fc \tag{12}$$

$$\frac{\partial c}{\partial t}+u\frac{\partial c}{\partial x}+v\frac{\partial c}{\partial y}=(D_c+D_{ct})\left(\frac{\partial^2 c}{\partial x^2}+\frac{\partial^2 c}{\partial y^2}\right)+\mathbf{S} \tag{13}$$

$$\frac{\partial T}{\partial t}+u\frac{\partial T}{\partial x}+v\frac{\partial T}{\partial y}=\frac{k_e+k_{et}}{\rho C_v}\left(\frac{\partial^2 T}{\partial x^2}+\frac{\partial^2 T}{\partial y^2}\right)+\frac{\mu}{\rho C_v}\left[\left(\frac{\partial u}{\partial y}+\frac{\partial v}{\partial x}\right)^2\right] \tag{14}$$

$$\frac{\partial k}{\partial t}+u_j\frac{\partial k}{\partial x_j}=\frac{\mu_t}{\rho}S^2-\epsilon+\frac{\partial}{\partial x_j}\left[\frac{1}{\rho}\left(\mu+\frac{\mu_t}{\sigma_k}\right)\frac{\partial k}{\partial x_j}\right] \tag{15}$$

$$\frac{\partial \epsilon}{\partial t}+u_j\frac{\partial \epsilon}{\partial x_j}=\frac{\epsilon}{k}\left(C_{1\epsilon}\frac{\mu_t}{\rho}S^2-C_{2\epsilon}\epsilon\right)+\frac{\partial}{\partial x_j}\left[\frac{1}{\rho}\left(\rho+\frac{\mu_t}{\sigma_\epsilon}\right)\frac{\partial \epsilon}{\partial x_j}\right] \tag{16}$$

In equations 15 and 16, there are five free constants which are; σ_k, σ_ϵ, $C_{1\epsilon}$, $C_{2\epsilon}$ and C_μ
These constants are determined on studying simple flows such as;

1. Decaying homogeneous isotropic turbulence with the constant $C_{2\epsilon}$
2. Homogeneous shear flow with the constants $C_{1\epsilon}$ and $C_{2\epsilon}$
3. The Logarithmic Layer constants $C_{1\epsilon}, C_{2\epsilon}, C_\mu, \sigma_k$ and σ_ϵ
4. Or by comparison with experimental data

Standard $k-\epsilon$ refers to a certain choice of the constants, and thus we consider this constants according to [10].

The viscous dissipation term in k-equation gives a negative contribution to equation due to the appearance of sum of squared fluctuating deformation rates. The dissipation of k is caused by work done by the smallest eddies against viscous stresses. The rate of dissipation per unit volume is normally written as the product of density ρ and the rate of dissipation of k per unit mass ϵ, i.e.

$$\epsilon=2v\overline{s'_{ij}\cdot s'_{ij}} \tag{17}$$

The dimensions of ϵ are m^2/s^3. This quantity is of vital importance in the study of turbulence dynamics. It is the destruction term in the turbulent kinetic energy equation, of a similar order of magnitude as the production term and never negligible.

4.1. Boundary and initial conditions for the mathematical model

Since the case is two-dimensional, the sides facing z-direction are set to zeros, which implies that no solution is required in that dimension (see figure 3). The sides facing flow direction are set as inlet,($x = 0$) and outlet,($x = x_N$) boundaries, which are given periodic boundary conditions. The boundary conditions at the wall are specified for each variable and considering no slip condition, the velocities ($u, v = 0$). Also at the side walls, given that there is no solid walls, the adiabatic boundary conditions were considered i.e. $\dfrac{\partial u}{\partial x} = 0$. This condition applied to all other flow variables including kinetic energy and dissipation. All these are set at the start of simulation for $t = 0$

4.2. Source function modeling

The source term in the lattice Boltzmann (LBGK) model scheme for convection–diffusion equation as proposed by [11] was used. They observed that unlike the models proposed previously, the present scheme only requires the source term in order of the Knudsen number by adding a differential operator of the source term to the evolution equation. The scheme can be applied to reaction–diffusion systems directly. Numerical results were found to be in excellent agreement with the analytical solutions.In this paper we used the LBGK scheme and represented the source function as in equation 18 below.

$$S(x, y, u, v) = \exp\left(-c\sqrt{(\mu_x)^2 + (\mu_y)^2}\right) t.\left[\sin \mu_x(1-x)\cosh \dot{\mu_y}(1-y)\right] \tag{18}$$

where, $\mu_x = \dfrac{u\pi}{L}$, $\mu_y = \dfrac{v\pi}{L}$ and c is a constant.

4.3. Surface roughness as a normal distribution function

Terrain features such as buildings, trees etc. are represented in some programs with the use of surface roughness; other programs include such features with the combination of 3D geometry and roughness. Surface roughness strongly affects wind flow separation and recirculation at hilly terrains [14]. Vertical mixing of a pollutant plume increases with surface roughness as mechanical turbulence exists over the ground. Common values exist for typical surfaces although most models use specific values that are known to work better according to each physical model employed. The surface roughness in the RANS equations represented as ***Smx*** and ***Smy*** were considered as normal distribution function in this paper. This function is as given in equation 19 . It act as a drug force to reduce the fluid velocity which in this case acts as a mitigating factor to the pollutants concentration along the field of consideration.

$$\boldsymbol{Smx}(x) = H * \tanh\left(\frac{(x - x_{on})}{x_s}\right) - \tanh\left(\frac{(x - x_{off})}{x_s}\right) \tag{19}$$

where H is the height of vegetation cover, x_{on} and x_{off} are the points of start and end of surface roughness cover and ***Smy*** $= H$.

5. Nondimensionalization of Governing Equations

The process of dimensional analysis is used to eliminate dimensions of variables involved in the model's governing equations. This process starts with selecting a suitable scale against which all dimensions in a given physical model are scaled. The process is of great generality and mathematical simplicity. This process aims at ensuring that the results obtained are applicable to other geometrically similar configurations under similar set of flow conditions.

To do this characteristic quantities were selected that described the flow problem, such as a characteristic length, L , characteristic velocity, U_∞ , characteristic pressure, p_∞, and characteristic temperature, T_∞.
Using these scaled quantities the following nondimensional parameters can be defined.

$$\begin{gathered} t^* = \frac{t}{\frac{L}{U_\infty}}, \quad x^* = \frac{x}{L}, \quad y^* = \frac{y}{L}, \quad z^* = \frac{z}{L} \\ , \quad u^* = \frac{u}{U_\infty}, \quad v^* = \frac{v}{U_\infty}, \quad w^* = \frac{w}{U_\infty}, \quad p^* = \frac{p - p_\infty}{\rho U_\infty^2}, \\ T^* = \frac{T - T_\infty}{\triangle T}, \quad C^* = \frac{C - C_\infty}{\triangle C}, \quad k^* = \frac{k - k_\infty}{\triangle k}, \quad \epsilon^* = \frac{\epsilon - \epsilon_\infty}{\triangle \epsilon} \end{gathered} \tag{20}$$

where $\triangle$ gives the reference flow variable difference in the flow parameters between a constant wall variable and maximum value i.e. $\triangle C$ is the reference pollutant concentration difference in the flow field such as the one between a constant wall concentration and C_∞. Using these definitions 20 in our specific governing equations 11 to 16, their non-dimensional forms were obtained as in equations 21 to 26

$$\frac{\partial u^*}{\partial t^*} + v^*\frac{\partial u^*}{\partial y^*} = -\frac{\partial p^*}{\partial x^*} + \left(\frac{1}{Re} + \frac{1}{Ret}\right)\left(\frac{\partial^2 u^*}{\partial x^{*2}} + \frac{\partial^2 u^*}{\partial y^{*2}}\right) + \frac{L}{U_\infty^2}\left(S_{mx} + fc\right) \tag{21}$$

$$\frac{\partial v^*}{\partial t^*} + v^* \frac{\partial v^*}{\partial y^*} = -\frac{\partial p^*}{\partial y^*} + \left(\frac{1}{Re} + \frac{1}{Ret}\right)\left(\frac{\partial^2 v^*}{\partial x^{*2}} + \frac{\partial^2 v^*}{\partial y^{*2}}\right) + \frac{L}{U_\infty^2}\left(S_{my} + fc\right) \tag{22}$$

$$\frac{\partial c^*}{\partial t^*} + u^* \frac{\partial c^*}{\partial x^*} + v^* \frac{\partial c^*}{\partial y^*} = \left(\frac{1}{Sc} + \frac{1}{Sct}\right)\left(\frac{\partial^2 c^*}{\partial x^{*2}} + \frac{\partial^2 c^*}{\partial y^{*2}}\right) + \frac{L}{U_\infty \triangle C}\mathbf{S} \tag{23}$$

$$\begin{aligned}\frac{\partial T^*}{\partial t^*} + u^* \frac{\partial T^*}{\partial x^*} + v^* \frac{\partial T^*}{\partial y^*} &= \left(\frac{1}{Pe} + \frac{1}{Pet}\right)\left(\frac{\partial^2 T^*}{\partial x^{*2}} + \frac{\partial^2 T^*}{\partial y^{*2}}\right) \\ &+ \frac{\mu U_\infty^2}{\rho C_v \triangle T L^2}\left(\frac{\partial u^*}{\partial y^*} + \frac{\partial v^*}{\partial x^*}\right)^2\end{aligned} \tag{24}$$

$$\begin{aligned}\frac{\partial k^*}{\partial t^*} + u^* \frac{\partial k^*}{\partial x^*} + v^* \frac{\partial k^*}{\partial y^*} &= \frac{\mu_t U_\infty}{\rho L \triangle k}\left(\frac{\partial u^*}{\partial y^*} + \frac{\partial v^*}{\partial x^*}\right)^2 - \left(\epsilon^* \cdot \triangle\epsilon + \epsilon_\infty\right)\frac{L}{U_\infty \triangle k} \\ &+ \left(\frac{\mu\sigma_k + \mu_t}{\rho\sigma_k L U_\infty}\right)\left[\frac{\partial^2 k^*}{\partial x^{*2}} + \frac{\partial^2 k^*}{\partial y^{*2}}\right]\end{aligned} \tag{25}$$

$$\begin{aligned}\frac{\partial \epsilon^*}{\partial t^*} + u^* \frac{\partial \epsilon^*}{\partial x^*} + v^* \frac{\partial \epsilon^*}{\partial y^*} &= \frac{\mu_t U_\infty C_{1\epsilon}}{\rho \triangle\epsilon}\left(\frac{\epsilon^* \cdot \triangle\epsilon + \epsilon_\infty}{k^* \cdot \triangle k + k_\infty}\right)\left(\frac{\partial u^*}{\partial y^*} + \frac{\partial v^*}{\partial x^*}\right)^2 \\ -\frac{L C_{2\epsilon}}{U_\infty \triangle\epsilon}\left(\frac{(\epsilon^* \cdot \triangle\epsilon + \epsilon_\infty)^2}{k^* \cdot \triangle k + k_\infty}\right) &+ \left(\frac{\mu\sigma_\epsilon + \mu_t}{\rho\sigma_\epsilon L U_\infty}\right)\left[\frac{\partial^2 \epsilon^*}{\partial x^{*2}} + \frac{\partial^2 \epsilon^*}{\partial y^{*2}}\right]\end{aligned} \tag{26}$$

The equations 21 to 26 were solved numerically by finite difference and Gauss-seidel approach using a MATLAB code subject the boundary and initial conditions as stated in the subsection herein. The temperature, kinetic energy, dissipation and concentration profiles were obtained.

6. Results and discussions

Agrochemical pollutants are carried by wind and their distribution in the environment mainly depends on the type and concentration of pollutants at a source, combined with prevailing weather and topographical conditions. The numerical scheme developed is implemented in MATLAB so as to obtain the approximate solutions. Temperature, kinetic energy, dissipation and concentration profiles distributions are discussed herein while parameters such as Reynolds, Peclet, Schmidt and Eckert numbers are being varied.

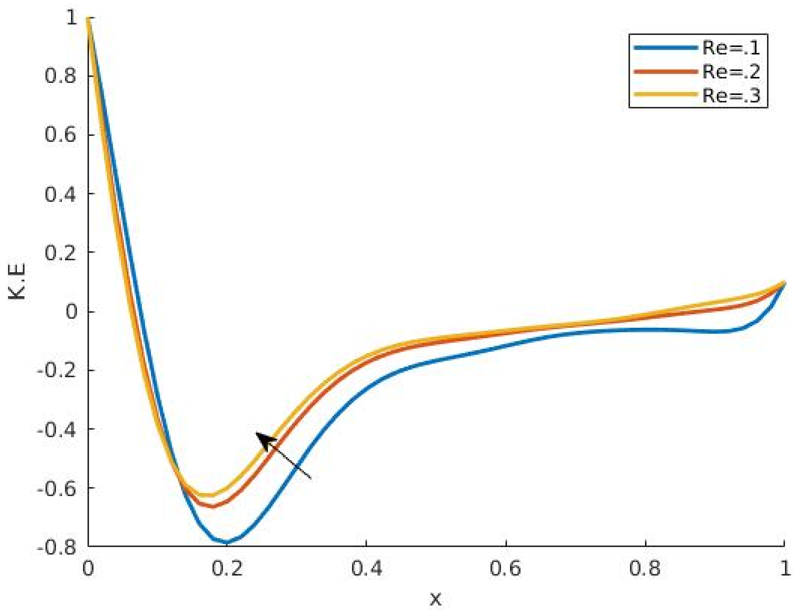

Fig. 4. Kinetic energy against the domain length(x) with varying Reynolds number (Re)

The wind velocity as it accesses the plantation is high but reduces within the area due to the vegetation cover as the sprayed agrochemicals diffuse in air. The Reynolds number (Re) helps predict flow patterns in different fluid flow situations where for this case we consider a turbulent flow. Figure 4 shows the variations of kinetic energy *KE* along the scope domain length while *Re* is being increased. Considering that the wind as carrier in this case, thus the increase in wind velocity, increases the kinetic energy which propels the dispersion of pollutants in the environment. It is observed that for increase in dynamic Reynolds number and turbulent Reynolds number, there is an increase of the kinetic energy *KE* along domain length. This is due to the fact that kinetic energy *KE* is a function of flow velocities and are directly related.

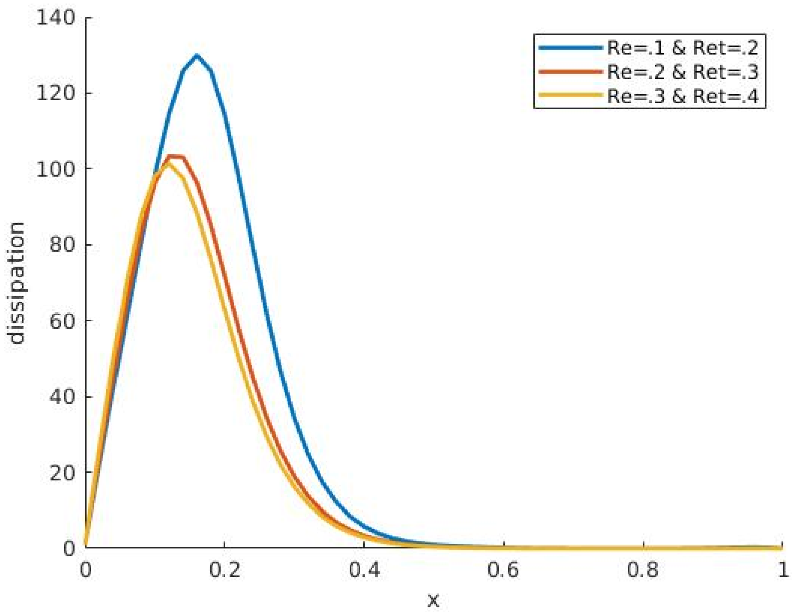

Fig. 5. Dissipation against the domain length(x) with varying Reynolds number (*Re*)

The dissipation of air pollutants is both a positive and negative occurrence. The positive effect of dissipation is that concentrations of harmful chemicals decrease as they spread across wider areas. The negative effect of dissipation is that the harmful chemicals are spread to other parts of the domain. Figure 5, shows the graph of dissipation rate (ϵ) against the domain length as Reynolds number in increases. Given that the Reynolds number (*Re*) is directly proportional to flow velocities, (ϵ) indicates the turbulence strength, which means it is usually higher where the TKE production is higher and this is as a result of increased flow velocities. This results are in agreement with [13]

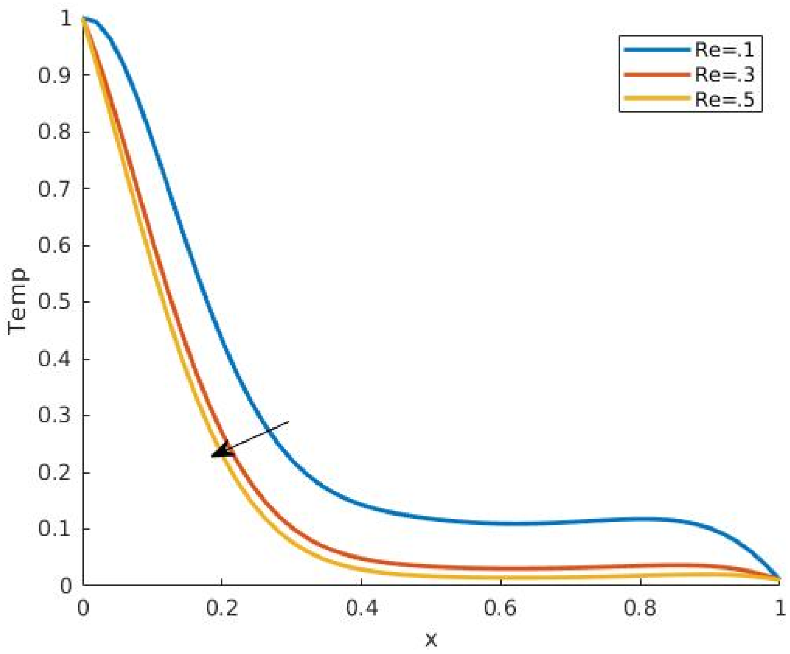

Fig. 6. Temperature against the domain length(x) with varying Reynolds number (*Re*)

The Reynolds number changes the inlet velocity of the fluid and a higher Reynolds number carries away heat faster. The heat flux changes while the influence on how the temperature of the fluid changes how the velocity profiles vary. From the figure 6, it is observed that the temperature reduces as the Reynolds number(*Re*) increases. This is due to the fact that higher Reynolds number carries away heat faster. When the flow is considered turbulent, the flow contains eddying motions of all sizes, and a large part of the mechanical energy in the flow goes into the formation of these eddies which eventually dissipate their energy as heat. This effect is minimal considering the horizontal dimension and hence small variation in temperature.

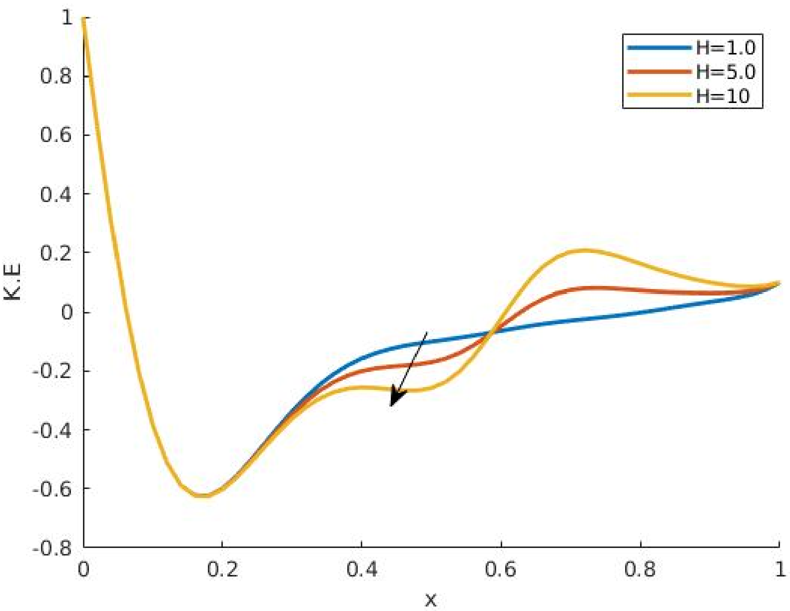

Fig. 7. Kinetic energy against the height of tress middle-way the area

Figure 7 shows the variations of *KE* along the scope domain while the trees height is being increased. The wind velocity as it accesses the plantation is high but reduces within the area due to the vegetation cover as the sprayed agrochemical pollutants diffuse in air. The *KE* is scaled at 1 at the beginning of the domain at $x = 0$ where the wind begin to encounter the vegetation. Considering that the wind as carrier in this case, thus the increase in wind velocity, increases the kinetic energy which propels the dispersion of pollutants in the environment. It is observed that at $x = .6$, with the increase in height of trees, the kinetic energy *KE*, reduces due to the reduced flow velocities as the trees act as a barrier to the wind. This in turn increases deposition of agrochemical pollutants where trees trap the particles. This results into reduced dispersion of the agrochemical pollutants to the residential areas and hence reduced incidences of chronic respiratory diseases.

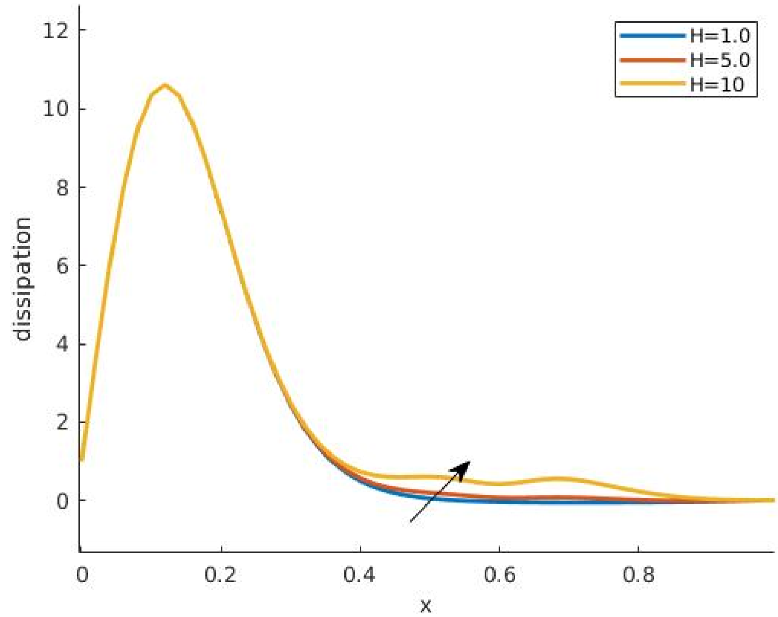

Fig. 8. Dissipation against the height of tress middle-way the area

Figure 8, shows the graph of dissipation against domain length where trees height vary. It is observed that dissipation rate increases with increase in trees height due to agrochemical pollutants deposition.

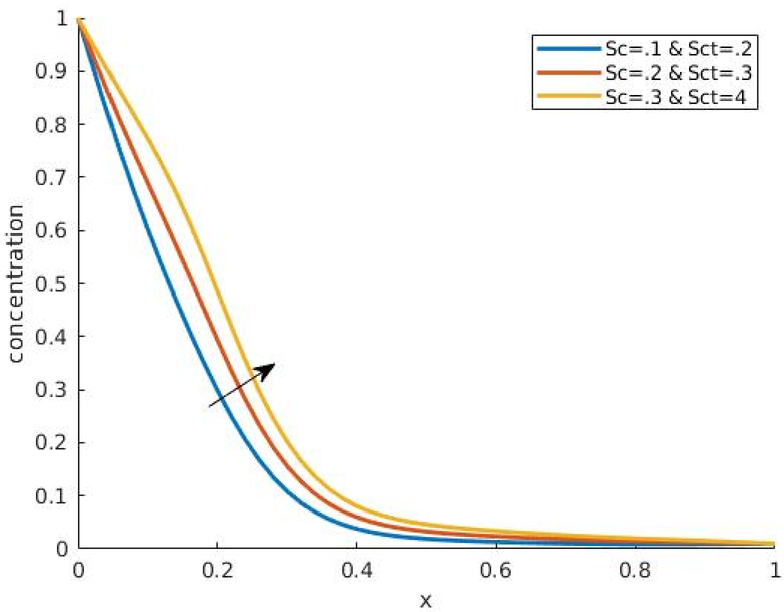

Fig. 9. Plot of pollutants concentration with varying Schmidt numbers

The variation of agrochemicals concentration with varying Schmidt numbers is observed as shown in figure 9. The Schmidt number (Sc) is the ratio of the kinematic viscosity to the molecular diffusion coefficient. A Schmidt number is used to characterize fluid flows in which there are simultaneous momentum and mass diffusion convection processes. From the figure 9, it is observed that as the Schmidt and turbulent Schmidt numbers decreased so does the pollutant concentration along the domain length. This implies that for small Schmidt number, pollutants diffusion dominates, whereas for high Schmidt numbers momentum diffusion will dominate.

7. Conclusion

In this paper we have successfully investigated air pollution due to agrochemicals over large farms by k-ϵ turbulence model. The results show that valid and reasonable solutions can be obtained by selecting the appropriate trees height to reduce the extent agrochemical pollution is felt. When the flow is considered turbulent, the flow contains eddying motions of all sizes, and a large part of the mechanical energy in the flow goes into the formation of these eddies which eventually dissipate their energy as heat. It can be conclude that, there is need for further study to discover the extent these chemicals can be barred from reaching the residential areas thus reducing the high risk of residents being affected by chronic respiratory diseases. Further research can be done over the vertical space of the atmospheric boundary layer. where forces as that of buoyancy can be introduced.

Acknowledgements

We gratefully acknowledge the support by Pan African University Institute of Basic Science, Technology and Innovation in financing this study, and supervisors Prof. Matthew Ngugi Kinyanjui and Dr. Eric Mark Mwiti Kimathi in guiding the work. Their supervision, support and patience were constant throughout the period of study. Their keen interest and understanding of the topic was inspiring and led to fruitful discussions.

References

[1] Hailu, Faris. "Farmers perception of pesticide use and genetic erosion of landraces of tetraploid wheat (Triticum spp.) in Ethiopia." Genetic resources and crop evolution 64 (2017): 979-994.
[2] Miraglia, Marina, H. J. P. Marvin, G. A. Kleter, Paola Battilani, C. Brera, E. Coni, F. Cubadda et al. "Climate change and food safety: an emerging issue with special focus on Europe." Food and chemical toxicology 47, no. 5 (2009): 1009-1021.
[3] Nadeem, Muhammad. "CONTRIBUTIONS TO THE STUDY OF SPRAYING OPERATIONS IN THE CONTEXT OF SUSTAINABLE AGRICULTURE." (2019).
[4] Oliveri Conti, Gea, Behzad Heibati, Itai Kloog, Maria Fiore, and Margherita Ferrante. "A review of AirQ Models and their applications for forecasting the air pollution health outcomes." Environmental Science and Pollution Research 24 (2017): 6426-6445.
[5] Cao, Junliang, Xuejiao Peng, and Dabo Xin. "Feasibility study of prescribed burning for crop residues based on urban air quality assessment." Journal of Environmental Management 317 (2022): 115480.
[6] Majewski, Michael S. Pesticides in the atmosphere: distribution, trends, and governing factors. Vol. 1. CRC press, 2019.
[7] Yan, Chenggong, Cong Niu, Shuai Ma, Haochao Tan, and Liming Xu. "CFD models as a tool to analyze the deformation behavior of grape leaves under an air-assisted sprayer." Computers and Electronics in Agriculture 198 (2022): 107112.
[8] Lee, Chern Han Sean, Swee King Phang, and Hou Kit Mun. "Design and implementation of an agricultural UAV with optimized spraying mechanism." In MATEC Web of Conferences, vol. 335, p. 02002. EDP Sciences, 2021.
[9] Chyrva, Illia. "Multicopter flow fields and their influence on a spray released from multicopters." (2021).
[10] Launder, Brian Edward, and Bahrat I. Sharma. "Application of the energy-dissipation model of turbulence to the calculation of flow near a spinning disc." Letters in heat and mass transfer 1, no. 2 (1974): 131-137.
[11] Shi, Baochang, Bin Deng, Rui Du, and Xingwang Chen. "A new scheme for source term in LBGK model for convection–diffusion equation." Computers and Mathematics with Applications 55, no. 7 (2008): 1568-1575.
[12] Tirado, M. Cristina, R. Clarke, L. A. Jaykus, A. McQuatters-Gollop, and J. M. Frank. "Climate change and food safety: A review." Food Research International 43, no. 7 (2010): 1745-1765.
[13] McCaffrey, Katherine, Laura Bianco, and James M. Wilczak. "Improved observations of turbulence dissipation rates from wind profiling radars." Atmospheric Measurement Techniques 10, no. 7 (2017): 2595-2611.
[14] Lun, Yu Fat, Akashi Mochida, Shuzo Murakami, Hiroshi Yoshino, and Taichi Shirasawa. "Numerical simulation of flow over topographic features by revised k–ϵ models." Journal of Wind Engineering and Industrial Aerodynamics

91, no.1 – 2 (2003): 231 – 245.